

## APPENDIX D ADDITIONAL VISUAL AND QUANTITATIVE RESULTS ON REAL-WORLD VISUAL DATA RESTORATION

In this appendix, we present additional visual and quantitative results concerning high-order tensor completion, high-order tensor RPCA, and hyperspectral tensor restoration tasks (mentioned in Sections V-B, V-C, and V-D, respectively).

### A. More Results on High-Order Tensor Completion Task

More visual inpainting results for order-4 hyperspectral videos of different sizes and scenes are illustrated in Fig. 10. The specific quantitative results under varying MR are reported in Table XIII. It can be observed that the proposed D-t-SVD method significantly enhances quantitative performance in typical random missing scenarios. For the often-occurring deadline missing in the spectral imaging, the latest high-order tensor decomposition-based approaches FCT-NFR, HTNN-DFT, and HTNN-DCT demonstrate exceptional completion capabilities, while our method achieves optimal average quantitative results across all MRs. We further present quantitative frame-wise PSNR and pixel-wise SAM in Fig. 11. Unmistakably, our method can yield satisfactory restoration results for different datasets, both spatially and spectrally. For inpainting results on order-4 color videos and order-5 light field images, we show the visual results obtained from their RGB frames/grids in Figs. 12 and 13, respectively, and the detailed comparative results of quantitative metrics are presented in Table XIV and Fig. 14, respectively. Consistent with the findings on hyperspectral video completion, both the visual and quantitative results on color videos and light field images demonstrate that our method achieves state-of-the-art performance in tensorized visual data inpainting, which validates the effectiveness of measuring the intrinsic global discrepancy of transformed high-order tensor singular values.

### B. More Results on High-Order Tensor RPCA Task

More representative visual denoising results obtained on various multi-dimensional visual datasets are shown in Fig. 15. It can be observed that the proposed method not only effectively removes sparse noise but also maintains optimal image details. We also report the specific quantitative results, frame-wise PSNR and pixel-wise SAM obtained on order-4 hyperspectral videos under three different NPs in Table XV and Fig. 16. Since our method avoids the bias issue inherent in convex optimization approaches, it delivers higher quantitative metric values when tackling more complex tensor RPCA tasks, both in terms of spatial and spectral aspects. More quantitative results for the remaining two types of multi-dimensional visual datasets are presented in Table XVI and Fig. 17. Another observation is that the LRTDGS method based on Tucker decomposition also achieves satisfactory results. The reason is that it further takes into account group smoothing priors. We can conclude that our method is more capable of restoring the clean component from sparsely degraded tensors, even if solely considering the global low-rank prior. When further considering other prior such as the above-mentioned group sparsity, or the piecewise smoothness and non-local

self-similarity, it is believed that our model would achieve comparable improvements in denoising results.

### C. More Results on Hyperspectral Tensor Restoration Task

We first specify the noisy cases that were added to the simulated hyperspectral image datasets, *i.e.*,

- **Case 1:** Zero-mean Gaussian noise with different standard deviations was added to all bands, and the variances were randomly selected from the interval [0.1, 0.2].
- **Case 2:** Same as case 1 but with the interval of [0.2, 0.3].
- **Case 3:** Same as case 1 but with the interval of [0.1, 0.3].
- **Case 4:** The Gaussian noise is added in the same way as Case 1. Furthermore, impulse noise with a density of 15% was added to 15% continuous bands.
- **Case 5:** The Gaussian noise is added in the same way as Case 1. Meanwhile, random stripes were added to 20 continuous bands and 10% of columns were contaminated.
- **Case 6:** The Gaussian noise is added in the same way as Case 1. Furthermore, random deadlines were added to 20 continuous bands and their number and width were randomly selected from [5, 10] and [1, 3], respectively.
- **Case 7:** Mixed noise of cases 1, 4, 5, and 6.

Quantitative results obtained from different perspectives are presented in Table XVII, Fig. 18, and Fig. 19, respectively, which validates the effectiveness and practical application values of our order- $d$  tensor D-t-SVD rank minimization regime and subspace low-rank learning. To provide a clearer observation of the intuitive mixed denoising results, we have included an enlarged version of Fig. 4, presented as Fig. 20. As this work is dedicated to improving the performance of high-order tensor rank approximation, we replaced the proposed D-t-SVD rank term in model (36) and developed two alternative models based on subspace low-rank learning, that is, S-WNNM based on matrix WNNM [1]:

$$\begin{aligned} & \min_{\mathbf{B}, \mathbf{C}} \frac{1}{2} \|\mathbf{Y} - \mathcal{T}(\mathbf{C} \times_3 \mathbf{B}) - \mathbf{\mathcal{E}}\|_F^2 + \gamma \sum_i \left\| \mathcal{R}_i(\mathbf{C})_{(2)} \right\|_{w,*} \\ & + \lambda \|\mathbf{\mathcal{E}}\|_{w,1}, \quad \text{s.t. } \mathbf{B}^T \mathbf{B} = \mathbf{I}, \end{aligned} \quad (1)$$

and S-HTNN based on high-order TNN [2]:

$$\begin{aligned} & \min_{\mathbf{B}, \mathbf{C}} \frac{1}{2} \|\mathbf{Y} - \mathcal{T}(\mathbf{C} \times_3 \mathbf{B}) - \mathbf{\mathcal{E}}\|_F^2 + \gamma \sum_i \left\| \mathcal{R}_i(\mathbf{C}) \right\|_{*,\mathcal{L}} \\ & + \lambda \|\mathbf{\mathcal{E}}\|_{w,1}, \quad \text{s.t. } \mathbf{B}^T \mathbf{B} = \mathbf{I}. \end{aligned} \quad (2)$$

From the reported results, one can observe that, compared to other tensor representation- and deep learning-based competitors, all three subspace-based models yield satisfactory denoising outcomes. Especially for severely degraded mixed noise cases, these three models achieve clear improvements both spatially and spectrally. Notably, the model equipped with our novel order- $d$  tensor low-rank measure, S-D-t-SVD, significantly enhances all quantitative metrics compared with the other two subspace-based models. This improvement is due to its deeper exploitation of the implicit high-order low-rank nature of hyperspectral image through the proposed D-t-SVD rank minimization regime, thereby easily achieving state-of-the-art results in an unsupervised manner. It's worth noting that

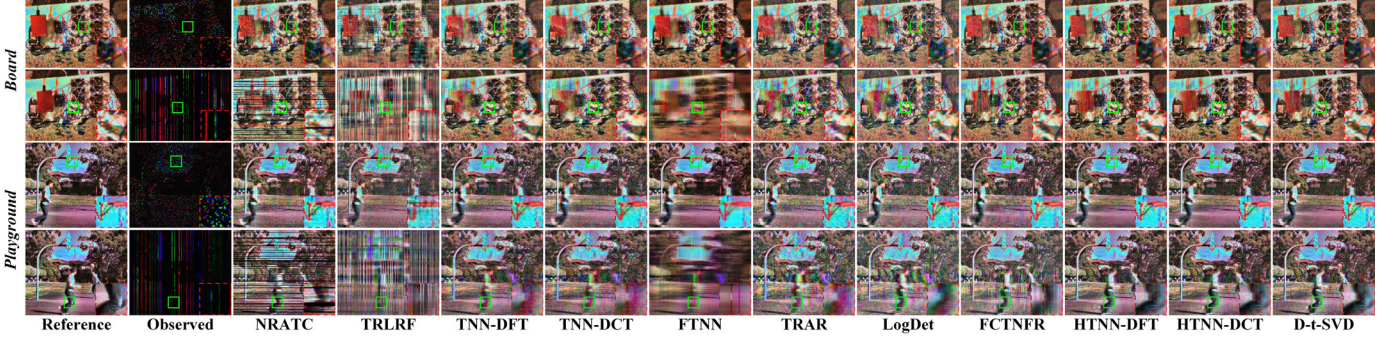


Fig. 10: Pseudo-color images of inpainting results with MR = 90% on order-4 **hyperspectral videos**.

TABLE XIII: Quantitative inpainting results comparison of all competing tensor completion methods on order-4 **hyperspectral videos** with different MRs. Hereinafter, the optimal and sub-optimal quantitative results are highlighted in **RED** and **GREEN**, respectively.

Missing Type	Dataset	MR	Index	NRATC	TRLRF	TNN-DFT	TNN-DCT	FTNN	TARA	LogDet	FCTNFR	HTNN-DFT	HTNN-DCT	D-t-SVD
Mian's	Board	80%	PSNR $\uparrow$	34.984	34.966	37.605	37.127	37.803	38.366	38.343	37.005	<b>39.178</b>	39.154	<b>40.124</b>
			SAM $\downarrow$	0.0643	0.0655	0.0444	0.0453	<b>0.0379</b>	0.0412	0.0442	0.0464	0.0401	0.0392	<b>0.0363</b>
			ERGAS $\downarrow$	3.1092	3.2000	2.3110	2.4568	2.3376	2.1107	2.1013	2.4913	<b>1.9230</b>	1.9234	<b>1.7107</b>
	Playground	90%	PSNR $\uparrow$	32.325	28.837	34.715	34.295	35.215	35.328	35.931	34.618	37.266	37.276	<b>38.229</b>
			SAM $\downarrow$	0.0790	0.1258	0.0571	0.0578	0.0452	0.0545	0.0554	0.0573	0.0477	0.0460	<b>0.0431</b>
			ERGAS $\downarrow$	4.2851	6.6668	3.2744	3.4639	3.2085	3.0501	2.8012	3.3786	<b>2.4210</b>	2.4122	<b>2.1353</b>
	Board	95%	PSNR $\uparrow$	26.990	23.794	31.803	31.631	32.299	28.937	32.827	31.672	33.860	34.088	<b>35.990</b>
			SAM $\downarrow$	0.1196	0.2000	0.0746	0.0739	0.0587	0.0998	0.0756	0.0751	0.0647	0.0600	<b>0.0518</b>
			ERGAS $\downarrow$	7.9606	11.498	4.6170	4.7412	4.4402	6.3043	4.0656	4.7380	3.6390	3.5650	<b>2.8042</b>
	Random missing	80%	PSNR $\uparrow$	35.102	27.068	30.718	30.642	32.167	31.660	32.044	33.709	36.204	36.293	<b>37.235</b>
			SAM $\downarrow$	0.0709	0.1734	0.0987	0.1003	0.0559	0.1071	0.1020	0.0713	<b>0.0522</b>	0.0523	<b>0.0521</b>
			ERGAS $\downarrow$	3.6687	9.2572	5.8957	5.9528	4.9749	5.2829	5.0544	4.1425	3.2561	3.1990	<b>2.8689</b>
		90%	PSNR $\uparrow$	28.866	23.288	26.965	27.046	28.386	27.820	27.732	31.153	32.197	<b>32.467</b>	<b>33.448</b>
			SAM $\downarrow$	0.1332	0.2504	0.1445	0.1440	0.0849	0.1554	0.1665	0.0934	0.0774	0.0762	<b>0.0743</b>
			ERGAS $\downarrow$	7.4227	14.129	9.0601	8.9893	7.6952	8.2096	8.2734	5.6024	5.0979	4.8930	<b>4.3624</b>
		95%	PSNR $\uparrow$	23.219	19.610	24.171	24.417	25.481	23.172	24.469	28.270	27.953	28.350	<b>30.103</b>
			SAM $\downarrow$	0.2077	0.3254	0.1848	0.1816	0.1180	0.2293	0.2333	0.1273	0.1221	0.1180	<b>0.1055</b>
			ERGAS $\downarrow$	13.943	20.941	12.460	12.133	10.743	13.935	12.040	7.8315	8.3052	<b>7.8110</b>	<b>6.3559</b>
	playground	80%	PSNR $\uparrow$	32.627	27.436	30.100	29.897	30.957	30.654	30.815	30.658	<b>34.601</b>	34.458	<b>35.577</b>
			SAM $\downarrow$	0.1018	0.1817	0.1312	0.1346	0.0940	0.1339	0.1310	0.1233	0.0745	0.0760	<b>0.0690</b>
			ERGAS $\downarrow$	4.7583	8.6853	6.1942	6.3345	5.6051	5.8219	5.7255	5.8166	3.7766	3.8390	<b>3.4036</b>
		90%	PSNR $\uparrow$	27.817	23.857	26.725	26.523	27.253	27.101	26.991	28.197	30.676	30.395	<b>31.547</b>
			SAM $\downarrow$	0.1709	0.2532	0.1896	0.1945	0.1444	0.2024	0.2097	0.1613	0.1134	0.1180	<b>0.1069</b>
			ERGAS $\downarrow$	8.1440	12.826	9.1142	9.3227	8.5541	8.7159	8.8227	7.7151	<b>5.8228</b>	6.0100	<b>5.2939</b>
		95%	PSNR $\uparrow$	22.673	20.510	24.425	24.261	24.584	23.288	24.281	25.609	26.779	26.415	<b>27.995</b>
			SAM $\downarrow$	0.2696	0.3335	0.2371	0.2424	0.1942	0.2869	0.2824	0.2103	0.1766	0.1850	<b>0.1607</b>
			ERGAS $\downarrow$	14.441	18.487	11.856	12.076	11.609	13.472	12.057	10.355	<b>9.0453</b>	9.4340	<b>7.8670</b>
	Mian's	80%	PSNR $\uparrow$	30.612	26.720	30.024	29.969	26.053	31.691	33.551	35.903	37.931	<b>38.245</b>	<b>39.426</b>
			SAM $\downarrow$	0.0937	0.1711	0.0840	0.0807	0.0960	0.0742	0.0647	0.0517	0.0447	0.0418	<b>0.0394</b>
			ERGAS $\downarrow$	5.2670	8.8451	5.6717	5.7437	8.9381	4.7795	3.7998	2.8352	2.2610	2.1437	<b>1.8494</b>
		90%	PSNR $\uparrow$	20.736	18.790	25.215	25.276	20.735	25.758	27.430	32.086	34.635	34.982	<b>37.269</b>
			SAM $\downarrow$	0.2421	0.3630	0.1385	0.1336	0.1662	0.1516	0.1260	0.0723	0.0597	0.0540	<b>0.0463</b>
			ERGAS $\downarrow$	16.196	21.084	9.8846	9.8728	16.527	9.6647	7.7341	4.4935	3.3492	3.1560	<b>2.3862</b>
		95%	PSNR $\uparrow$	14.326	14.573	21.712	21.672	13.446	19.251	22.411	28.691	28.292	28.719	<b>33.173</b>
			SAM $\downarrow$	0.5090	0.4979	0.2019	0.1994	0.3934	0.2982	0.2292	0.0913	0.1090	0.0947	<b>0.0653</b>
			ERGAS $\downarrow$	33.238	33.744	14.741	14.877	37.755	20.684	13.771	6.5692	6.9660	6.5380	<b>3.8806</b>
	Deadlines missing	80%	PSNR $\uparrow$	25.924	21.005	25.518	26.455	21.190	27.524	27.914	32.480	34.312	34.750	<b>35.865</b>
			SAM $\downarrow$	0.1804	0.3234	0.1417	0.1344	0.1586	0.1529	0.1452	0.0849	<b>0.0601</b>	<b>0.0591</b>	0.0616
			ERGAS $\downarrow$	10.885	18.650	11.154	9.911	17.772	8.7324	8.2780	4.8645	4.0437	3.7880	<b>3.3377</b>
		90%	PSNR $\uparrow$	17.543	15.513	21.875	22.723	16.886	23.241	23.515	29.096	29.932	30.721	<b>31.782</b>
			SAM $\downarrow$	0.4386	0.4928	0.1996	0.1913	0.2296	0.2286	0.2391	0.1271	0.0916	<b>0.0872</b>	0.0882
			ERGAS $\downarrow$	27.193	34.133	16.963	15.211	28.741	14.528	13.955	7.3073	6.7312	5.9870	<b>5.2682</b>
		95%	PSNR $\uparrow$	13.195	13.086	19.267	19.840	13.367	18.507	19.841	23.905	25.673	26.495	<b>28.346</b>
			SAM $\downarrow$	0.7138	0.5837	0.2567	0.2489	0.3692	0.3467	0.3398	0.3104	0.1452	0.1370	<b>0.1285</b>
			ERGAS $\downarrow$	43.891	45.276	22.745	21.188	42.935	25.218	21.421	15.156	10.992	<b>9.7440</b>	<b>7.8316</b>
	playground	80%	PSNR $\uparrow$	24.600	20.795	26.720	26.342	24.584	26.833	27.741	29.649	33.264	32.940	<b>34.675</b>
			SAM $\downarrow$	0.1971	0.3585	0.1767	0.1846	0.1942	0.1907	0.1722	0.1380	0.0838	0.0866	<b>0.0758</b>
			ERGAS $\downarrow$	11.832	18.6188	9.2349	9.6380	11.6091	9.0818	8.1772	6.5634	4.3619	4.5220	<b>3.7631</b>
		90%	PSNR $\uparrow$	16.878	15.561	23.681	23.341	19.516	23.446	24.045	25.609	29.135	28.546	<b>30.005</b>
			SAM $\downarrow$	0.4583	0.5068	0.2492	0.2598	0.2782	0.2899	0.2733	0.2103	<b>0.1309</b>	0.1400	<b>0.1251</b>
			ERGAS $\downarrow$	28.240	33.584	13.031	13.541	20.950	13.423	12.435	10.355	<b>6.9241</b>	7.4040	<b>6.2834</b>
		95%	PSNR $\uparrow$	12.944	13.049	21.311	20.965	14.900	19.496	21.268	21.830	25.196	24.655	<b>26.069</b>
			SAM $\downarrow$	0.7468	0.5620	0.3153	0.3293	0.4004	0.3780	0.3160	0.2067	0.2210	0.1963	<b>0.1963</b>
			ERGAS $\downarrow$	44.140	44.875	17.304	17.987	36.558	21.991	17.260	16.226	10.857	11.590	<b>9.7901</b>

to highlight the superiority of our novel rank minimization, we deliberately chose not to consider other advanced priors to the model. For example, further considering the orientational sensitivity of the t-SVD framework [3], the continuity of the spectral basis [4], or the smoothness of multiple dimensions [5] could result in further improved results.

Meanwhile, the real-world hyperspectral image denoising results on the *Urban* dataset obtained by the well-known HYDICE sensor are shown in Fig. 21. Few methods can effectively restore the most severely degraded bands. It is evident that even for these bands, the proposed S-D-t-SVD method effectively removes the tanglesome noise generated in the real-world imaging process. Compared with S-WNNM

and S-HTNN, which are also based on the subspace low-rank learning framework, the proposed S-D-t-SVD more effectively recovers the low-rank clean image from the stripe degradation caused by the push-broom hyperspectral imaging mechanism, demonstrating superior practical application value.

## REFERENCES

- [1] S. Gu, Q. Xie, D. Meng, W. Zuo, X. Feng, and L. Zhang, “Weighted nuclear norm minimization and its applications to low level vision,” *Int. J. Comput. Vis.*, vol. 121, pp. 183–208, 2017.
- [2] W. Qin, H. Wang, F. Zhang, J. Wang, X. Luo, and T. Huang, “Low-rank high-order tensor completion with applications in visual data,” *IEEE Trans. Image Process.*, vol. 31, pp. 2433–2448, 2022.
- [3] Y.-B. Zheng, T.-Z. Huang, X.-L. Zhao, T.-X. Jiang, T.-H. Ma, and T.-Y. Ji, “Mixed noise removal in hyperspectral image via low-fibered-rank

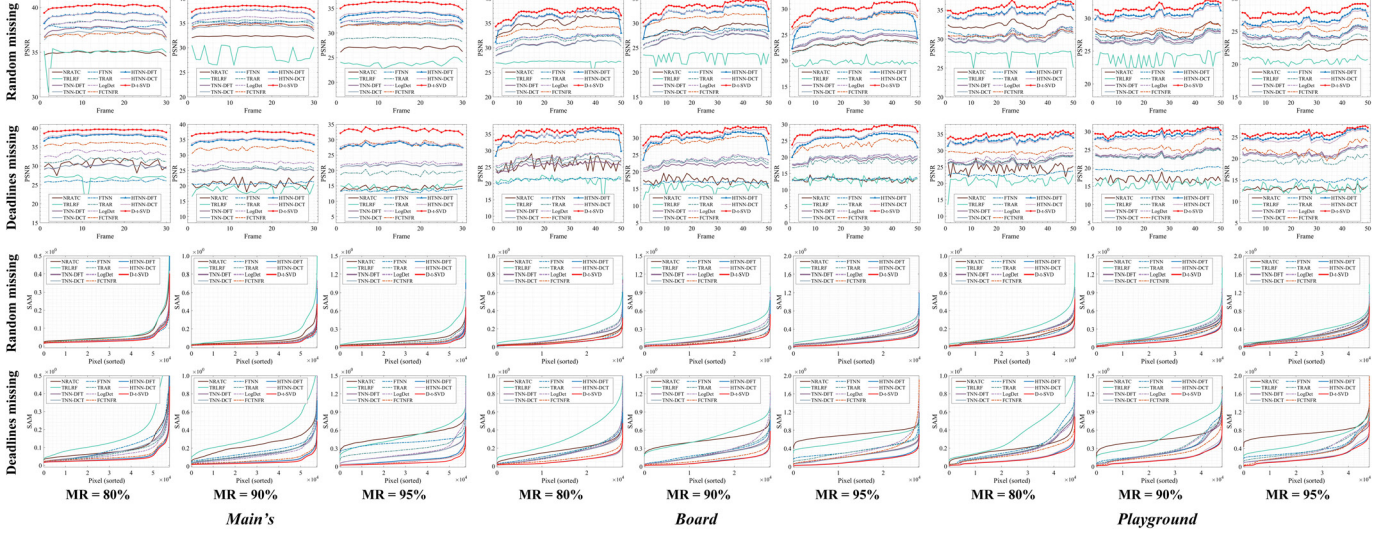


Fig. 11: PSNR as a function of frames (upper) and SAM (plotted in a  $\log_{10}(\bullet)$  scale, bottom) as a function of sorted pixels on order-4 hyperspectral videos with different MRs of random missing and deadlines missing.



Fig. 12: RGB frame images of inpainting results with  $MR = 80\%$  on order-4 color videos.

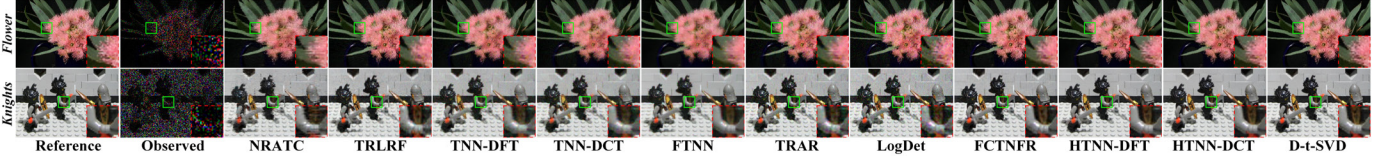


Fig. 13: RGB grid images of inpainting results with  $MR = 80\%$  on order-5 light field images.

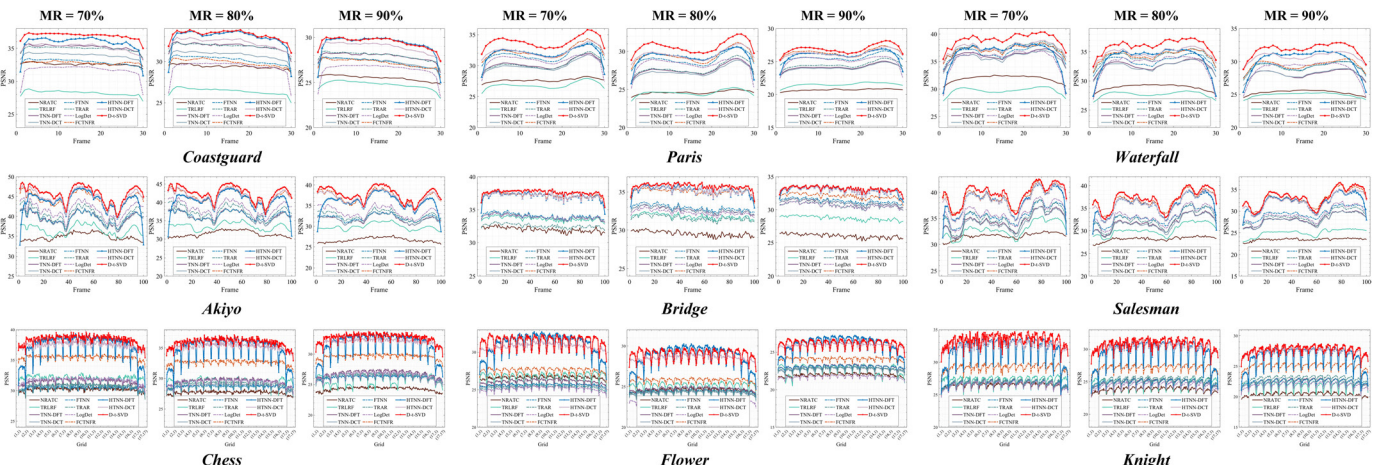


Fig. 14: PSNR as a function of RGB frames/grids on order-4 color videos and order-5 light field images with different MRs.

TABLE XIV: Quantitative inpainting results comparison of all competing tensor completion methods on order-4 **color videos** and order-5 **light field images** with different MRs.

Data type	Dataset	MR	Index	NRATC	TRLRF	TNN-DFT	TNN-DCT	FTNN	TARA	LogDet	FCTNFR	HTNN-DFT	HTNN-DCT	D-t-SVD
order-4 color video (CIF format)	Coastguard	70%	PSNR↑	32.594	28.228	35.142	33.916	32.918	34.928	31.657	32.799	<b>35.762</b>	35.132	<b>36.914</b>
		80%	ERGAS↓	3.4201	5.6585	2.5584	2.9438	3.3005	2.6177	3.9053	3.3401	<b>2.4478</b>	2.5634	<b>2.0850</b>
		90%	PSNR↑	25.491	24.735	27.885	27.238	27.242	27.959	26.426	27.133	<b>29.244</b>	28.923	<b>29.442</b>
	Paris	70%	ERGAS↓	4.9454	6.9992	3.7422	4.2309	4.5251	3.7519	5.1023	4.6977	<b>3.4142</b>	3.5669	<b>3.1985</b>
		80%	PSNR↑	27.652	26.835	30.294	30.001	31.761	30.247	30.826	32.274	31.989	<b>32.336</b>	<b>33.860</b>
		90%	ERGAS↓	6.8297	7.5290	5.0883	5.2602	4.3083	5.1293	4.8477	4.0650	4.2439	<b>4.0316</b>	<b>3.3959</b>
	Waterfall	70%	PSNR↑	24.605	24.572	27.608	27.389	28.979	27.771	28.269	29.455	29.270	<b>29.622</b>	<b>30.652</b>
		80%	ERGAS↓	9.6802	9.7405	6.9090	7.0828	5.9072	6.7996	6.4675	5.6306	5.7685	<b>5.4869</b>	<b>4.8902</b>
		90%	PSNR↑	20.707	21.515	24.181	24.073	25.612	24.513	25.146	<b>26.369</b>	25.920	26.236	<b>26.912</b>
order-4 color video (QCIF format)	Akiyo	70%	PSNR↑	31.893	29.672	36.091	35.754	36.630	37.398	35.439	37.128	36.477	<b>37.538</b>	<b>39.003</b>
		80%	ERGAS↓	4.4732	5.7807	2.8288	2.9351	2.6682	2.4516	3.2558	2.5337	2.9413	<b>2.4046</b>	<b>2.0606</b>
		90%	PSNR↑	6.2726	7.1974	4.1449	4.2317	3.7952	3.5015	4.3171	3.4642	3.8842	<b>3.2672</b>	<b>2.8680</b>
	Bridge	70%	PSNR↑	28.891	27.693	32.668	32.493	33.451	34.221	32.822	34.391	33.829	<b>34.781</b>	<b>36.030</b>
		80%	ERGAS↓	9.4223	9.8185	6.9099	6.8724	6.0353	6.1491	6.6075	5.9229	5.6601	<b>5.1253</b>	<b>4.5839</b>
		90%	PSNR↑	34.823	36.539	39.503	39.422	39.655	40.518	41.606	44.313	43.659	<b>44.823</b>	<b>45.744</b>
	Salesman	70%	ERGAS↓	2.9754	2.4743	1.7841	1.8022	1.7448	1.6037	1.4203	1.0313	1.2166	<b>0.9910</b>	<b>0.8950</b>
		80%	PSNR↑	31.437	33.488	36.283	36.256	36.477	37.483	38.485	<b>41.693</b>	40.494	41.648	<b>42.640</b>
		90%	ERGAS↓	4.3876	3.4837	2.5550	2.5649	2.4878	2.2502	2.0216	1.3911	1.7068	1.4122	<b>1.2655</b>
order-5 light field image	Chess	70%	PSNR↑	31.999	33.627	33.903	33.937	34.086	32.545	33.884	35.961	37.037	<b>37.084</b>	<b>37.616</b>
		80%	ERGAS↓	3.0749	2.5670	2.4726	2.4625	2.4213	2.8882	2.4758	2.6764	1.7403	1.7258	<b>1.6199</b>
		90%	PSNR↑	29.526	31.793	32.629	32.659	32.926	31.565	32.304	33.702	35.196	<b>35.224</b>	<b>35.748</b>
	Flowers	70%	PSNR↑	26.030	28.728	31.049	31.087	31.336	30.664	30.648	30.601	32.936	<b>32.948</b>	<b>33.182</b>
		80%	ERGAS↓	6.1097	4.4827	3.4369	3.4215	3.3222	3.5899	3.5958	4.9417	2.7816	<b>2.7727</b>	<b>2.6949</b>
		90%	PSNR↑	31.625	32.889	34.448	34.180	35.648	35.100	36.006	<b>39.139</b>	38.359	38.579	<b>39.697</b>
	Knights	70%	ERGAS↓	4.8351	4.2803	3.6136	3.7385	3.1372	3.3901	3.0357	<b>2.1241</b>	2.3927	2.3054	<b>2.0157</b>
		80%	PSNR↑	28.174	30.201	31.788	31.569	33.060	32.554	33.179	<b>36.657</b>	35.702	35.953	<b>36.967</b>
		90%	ERGAS↓	7.1815	5.8000	4.8927	5.0274	4.2207	4.5279	4.2030	<b>4.8207</b>	3.2231	3.1072	<b>2.7787</b>
	Bridge	70%	PSNR↑	30.230	31.967	31.487	30.594	30.425	30.708	31.706	35.437	37.266	<b>37.501</b>	<b>38.391</b>
		80%	ERGAS↓	5.3486	4.3950	4.6399	5.1381	5.2319	5.0718	4.5190	2.9422	2.5244	<b>2.3283</b>	<b>2.1092</b>
		90%	PSNR↑	7.1601	5.9373	5.8453	6.4138	6.4655	6.5732	5.8729	4.0698	3.3176	<b>3.0315</b>	<b>2.7969</b>
	Salesman	70%	PSNR↑	26.637	26.805	26.110	25.536	25.625	23.705	25.132	27.598	<b>31.071</b>	30.780	<b>31.470</b>
		80%	ERGAS↓	9.7682	9.6335	10.421	11.121	10.993	13.757	11.6800	8.7775	<b>6.0418</b>	6.0984	<b>5.6728</b>
		90%	PSNR↑	24.278	25.879	26.807	26.138	26.156	26.202	26.609	29.608	31.601	<b>32.018</b>	<b>32.694</b>
	Waterfall	70%	PSNR↑	21.986	22.783	23.067	22.697	23.067	21.923	21.725	24.092	<b>26.084</b>	25.958	<b>26.193</b>
		80%	ERGAS↓	16.663	15.299	14.759	15.391	14.739	16.849	17.259	13.118	<b>10.578</b>	10.598	<b>10.349</b>
		90%	PSNR↑	26.477	27.295	26.792	26.614	26.806	26.081	26.533	29.190	31.819	<b>32.586</b>	<b>33.267</b>
	Paris	70%	PSNR↑	8.6379	7.5417	7.6165	7.7325	7.5711	6.6511	8.0134	5.8799	4.6875	<b>4.1035</b>	<b>3.8544</b>
		80%	ERGAS↓	20.392	21.888	22.456	22.377	22.487	22.582	21.971	24.984	26.498	<b>27.316</b>	<b>27.952</b>
		90%	PSNR↑	12.778	10.792	10.097	10.188	10.050	9.9438	10.668	7.5466	6.5690	<b>5.7735</b>	<b>5.3920</b>

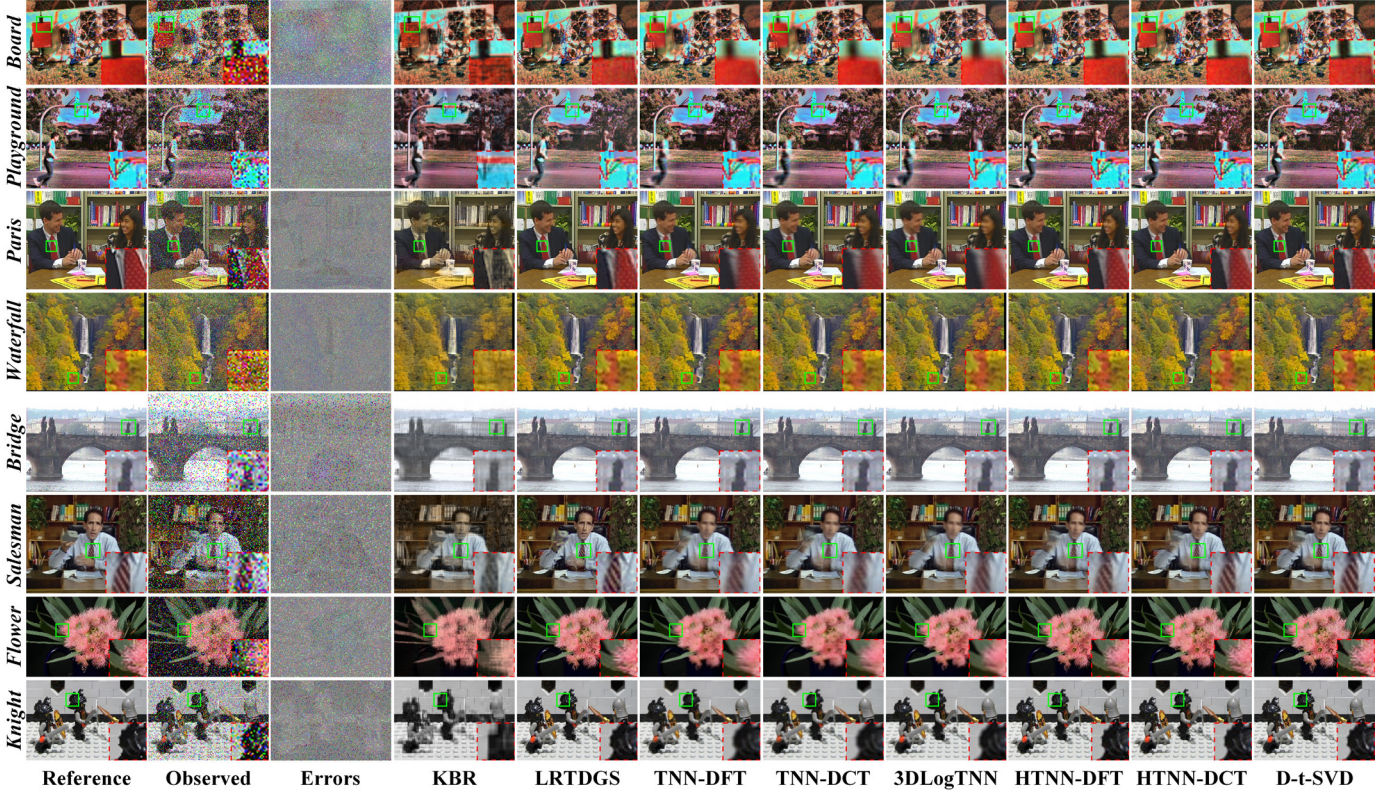


Fig. 15: Denoising results with NP = 20% on the 10-th frame of order-4 **hyperspectral/color videos** and the (10, 10)-grid of order-5 **light field images**.

TABLE XV: Quantitative denoising results comparison of all competing tensor RPCA methods on order-4 **hyperspectral videos** with different NPs.

Dataset	NP	KBR	LRTDGS				TNN-DFT				TNN-DCT				3DLogTNN				HTNN-DFT				HTNN-DCT				D-t-SVD	
		PSNR↑	SAM↓	ERGAS↓	PSNR↑	SAM↓	ERGAS↓	PSNR↑	SAM↓	ERGAS↓	PSNR↑	SAM↓	ERGAS↓	PSNR↑	SAM↓	ERGAS↓	PSNR↑	SAM↓	ERGAS↓	PSNR↑	SAM↓	ERGAS↓	PSNR↑	SAM↓	ERGAS↓	PSNR↑	SAM↓	ERGAS↓
Mian's board	0.1	33.984	0.0670	3.9394	<b>39.032</b>	0.0405	<b>2.0954</b>	37.993	0.0354	2.3694	37.567	0.0361	2.5310	37.519	<b>0.0329</b>	2.7864	38.749	0.0360	2.1258	38.372	0.0356	2.2879	<b>42.326</b>	<b>0.0297</b>	<b>1.3266</b>			
	0.2	33.162	0.0744	4.4835	37.889	0.0510	2.5955	37.376	0.0374	2.5483	36.978	0.0382	2.7089	36.738	0.0377	2.9982	<b>38.210</b>	0.0376	<b>2.2753</b>	37.890	<b>0.0370</b>	2.4308	<b>41.300</b>	<b>0.0321</b>	<b>1.5046</b>			
	0.3	32.318	0.0815	4.9900	36.086	0.0580	2.9567	36.625	0.0402	2.7749	36.255	0.0411	2.9365	35.807	0.0433	3.2835	<b>37.564</b>	0.0398	<b>2.4594</b>	37.302	<b>0.0389</b>	2.6083	<b>39.948</b>	<b>0.0362</b>	<b>1.7764</b>			
playground	0.1	27.473	0.1417	9.1023	35.266	0.0601	3.6727	30.755	0.0572	5.9936	30.662	0.0572	6.0823	31.879	0.0518	5.2583	<b>38.217</b>	0.0387	2.7146	34.038	0.0380	2.6750	<b>41.723</b>	<b>0.0327</b>	<b>1.6964</b>			
	0.2	26.197	0.1541	10.223	34.349	0.0747	4.1876	29.845	0.0639	6.6444	29.784	0.0640	6.7160	31.197	0.0621	5.6666	34.997	0.0463	4.0888	<b>35.022</b>	0.0444	3.7985	<b>39.624</b>	<b>0.0409</b>	<b>2.1610</b>			
	0.3	24.452	0.1731	12.156	33.012	0.0822	4.8436	28.850	0.0726	7.4445	28.807	0.0728	7.5018	30.210	0.0758	6.3180	33.672	0.0581	4.7114	<b>33.767</b>	0.0556	4.3500	<b>37.626</b>	<b>0.0516</b>	<b>2.7093</b>			
	0.1	25.958	0.1663	10.341	32.553	0.0955	5.0075	28.005	0.1143	7.8767	27.762	0.1181	8.0970	28.331	0.1134	7.5660	35.850	<b>0.0678</b>	3.2727	<b>35.886</b>	0.0682	<b>3.2567</b>	<b>40.231</b>	<b>0.0436</b>	<b>2.0136</b>			
	0.2	25.658	0.1727	10.674	<b>32.148</b>	<b>0.1027</b>	5.1637	27.367	0.1246	8.4805	27.105	0.1291	8.7384	27.898	0.1250	7.9508	32.117	0.1078	<b>4.9379</b>	31.974	0.1103	5.0152	<b>38.118</b>	<b>0.0539</b>	<b>2.5535</b>			
	0.3	25.092	0.1805	11.259	<b>31.103</b>	0.1196	<b>5.6686</b>	26.677	0.1372	9.1871	26.407	0.1423	9.4779	27.568	0.1360	8.2524	29.542	<b>0.1085</b>	6.7436	29.143	0.1122	7.1207	<b>36.757</b>	<b>0.0655</b>	<b>2.9674</b>			

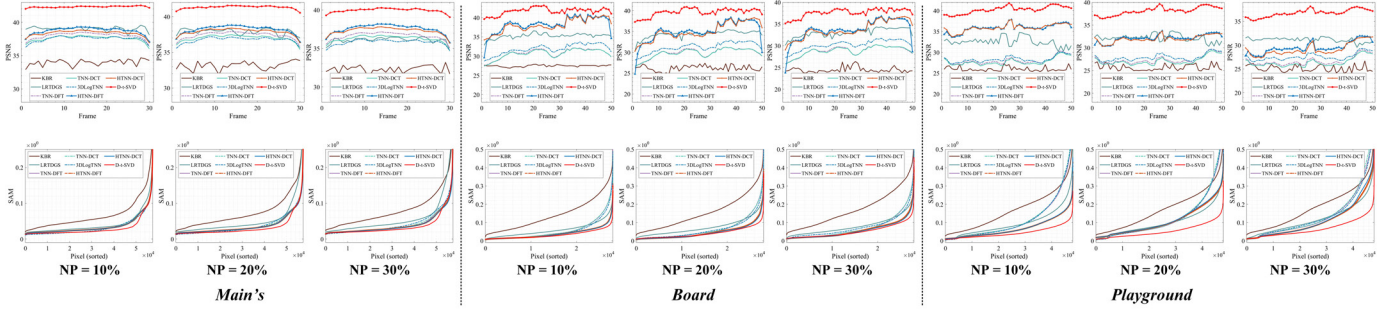


Fig. 16: PSNR as a function of frames (upper) and SAM (plotted in a  $\log_{10}(\bullet)$  scale, bottom) as a function of sorted pixels on order-4 **hyperspectral videos** with different NPs.

TABLE XVI: Quantitative denoising results comparison of all competing tensor RPCA methods on order-4 **color videos** and order-5 **light field images** with different NPs.

Data Type	Dataset	NP	KBR		LRTDGS		TNN-DFT		TNN-DCT		3DLogTNN		HTNN-DFT		HTNN-DCT		D-t-SVD	
			PSNR↑	ERGAS↓	PSNR↑	ERGAS↓	PSNR↑	ERGAS↓	PSNR↑	ERGAS↓	PSNR↑	ERGAS↓	PSNR↑	ERGAS↓	PSNR↑	ERGAS↓	PSNR↑	ERGAS↓
order-4 color video (CIF format)	Coastguard	0.1	34.980	2.6163	36.024	2.3369	34.146	2.8983	34.575	2.7933	33.223	3.2243	38.135	1.8366	<b>38.142</b>	1.8659	<b>41.623</b>	<b>1.2101</b>
		0.2	32.719	3.3824	31.273	3.9889	33.047	3.2847	33.150	3.2699	31.890	3.7473	34.769	2.6954	34.793	2.7196	<b>37.782</b>	<b>1.8874</b>
		0.3	29.857	4.6976	28.980	5.2146	31.705	3.8262	31.607	3.8389	30.292	4.4939	32.469	3.5048	32.471	3.5237	34.098	<b>2.9127</b>
order-4 color video (QCIF format)	Paris	0.1	21.996	13.656	32.490	3.9838	27.790	6.7845	27.617	6.9183	27.325	7.1907	33.292	3.6351	33.260	3.6406	<b>36.972</b>	<b>2.3910</b>
		0.2	21.155	14.907	<b>30.405</b>	<b>5.0421</b>	27.158	7.2812	27.016	7.4004	26.876	7.5619	29.873	5.3490	29.814	5.3806	<b>32.934</b>	<b>3.7831</b>
		0.3	20.118	16.650	<b>28.438</b>	5.6873	26.502	7.8398	26.381	7.9502	26.397	7.9809	28.307	6.3821	28.219	6.4469	<b>30.453</b>	<b>5.0167</b>
order-4 color video (QCIF format)	Waterfall	0.1	27.413	7.8506	38.510	2.1559	36.672	2.6575	37.274	2.5477	37.314	2.5088	40.110	1.7317	40.202	<b>1.7265</b>	<b>42.201</b>	<b>1.4166</b>
		0.2	25.941	9.2677	36.125	2.8273	35.285	3.1208	35.705	3.0419	36.439	3.2732	37.372	2.3627	<b>37.411</b>	2.3818	<b>39.368</b>	<b>1.9532</b>
		0.3	24.609	10.642	33.661	4.1352	33.663	3.7574	33.948	3.9686	<b>35.400</b>	3.1184	34.917	3.1361	35.099	<b>3.0986</b>	<b>37.180</b>	<b>2.4977</b>
order-4 color video (QCIF format)	Akiyo	0.1	26.178	8.5649	<b>41.678</b>	<b>1.8142</b>	34.555	3.1442	34.660	3.1148	34.266	3.2642	39.565	2.2542	39.487	2.0077	<b>45.126</b>	<b>0.9974</b>
		0.2	23.985	12.055	37.431	3.5878	33.747	3.4279	33.827	3.4043	33.610	3.5043	38.444	2.4898	38.418	2.2115	<b>42.780</b>	<b>1.2946</b>
		0.3	21.932	15.733	36.611	4.5105	32.903	3.7556	32.930	3.7524	32.915	3.7764	36.024	2.8128	36.979	2.5092	<b>41.192</b>	<b>1.5098</b>
order-5 Light field image	Bridge	0.1	27.014	5.4776	35.496	2.0818	33.243	2.6742	33.312	2.6524	31.882	3.1246	38.953	1.9913	36.007	1.9532	<b>39.157</b>	<b>1.3562</b>
		0.2	26.300	5.9434	32.811	3.5534	32.904	2.7809	32.963	2.7614	31.774	3.1640	34.688	2.2709	34.806	2.2380	<b>37.611</b>	<b>1.6201</b>
		0.3	25.569	6.4596	31.214	4.5774	32.537	2.8997	32.586	2.8832	31.670	3.2026	37.439	33.121	37.714	35.653	<b>2.0344</b>	
order-5 Light field image	Salesman	0.1	25.373	9.9797	35.718	3.0978	33.278	4.2129	33.042	4.3457	32.161	4.7894	37.288	3.0766	<b>37.476</b>	<b>2.9583</b>	<b>41.897</b>	<b>1.5646</b>
		0.2	24.327	11.243	34.471	3.9244	32.383	4.6535	32.155	4.7946	31.597	5.1083	35.591	3.5299	35.925	3.3847	<b>39.297</b>	<b>2.1546</b>
		0.3	23.133	12.882	32.734	5.5663	31.462	5.1517	31.249	5.2982	30.923	5.5148	34.429	4.2579	<b>33.749</b>	<b>4.0965</b>	<b>37.049</b>	<b>2.7754</b>
order-5 Light field image	Chess	0.1	26.820	7.9391	33.586	3.6802	28.342	6.6644	27.685	7.1848	28.776	6.3270	<b>34.548</b>	<b>3.3627</b>	34.244	3.3730	<b>40.286</b>	<b>1.6953</b>
		0.2	26.235	8.4882	<b>32.568</b>	4.3150	27.859	7.0478	27.193	7.0603	28.466	6.5583	32.368	4.3105	<b>32.199</b>	4.2646	<b>37.844</b>	<b>2.2523</b>
		0.3	25.625	9.1019	<b>31.133</b>	4.9085	27.311	7.5088	26.650	8.0966	28.114	6.8311	30.487	5.3731	31.073	<b>4.8562</b>	<b>35.204</b>	<b>3.0307</b>
order-5 Light field image	Flowers	0.1	23.316	14.404	28.543	7.8677	24.736	12.175	24.252	12.866	24.365	12.715	32.614	5.1499	33.379	4.5211	<b>36.827</b>	<b>3.0558</b>
		0.2	22.737	15.365	27.239	9.1441	24.403	12.647	23.957	13.307	24.136	13.050	28.229	8.3372	29.223	7.2763	<b>32.161</b>	<b>5.2109</b>
		0.3	22.103	16.491	26.132	10.386	24.069	13.141	23.663	13.764	23.927	13.365	27.278	9.2594	27.179	8.6497	<b>29.693</b>	<b>6.9167</b>
order-5 Light field image	Knights	0.1	21.309	11.640	30.417	4.0493	25.603	7.0458	25.444	7.1746	25.918	6.7873	33.459	2.9864	<b>33.613</b>	2.8030	<b>37.086</b>	<b>1.8902</b>
		0.2	20.505	12.668	29.211	4.6549	25.059	7.5023	24.908	7.6321	25.533	7.0957	30.403	4.2219	30.359	3.9900	<b>33.325</b>	<b>2.9044</b>
		0.3	19.979	13.412	27.960	5.3588	24.464	8.0335	24.328	8.1584	25.205	7.3670	28.103	5.6017	28.588	4.9853	<b>31.300</b>	<b>3.6677</b>

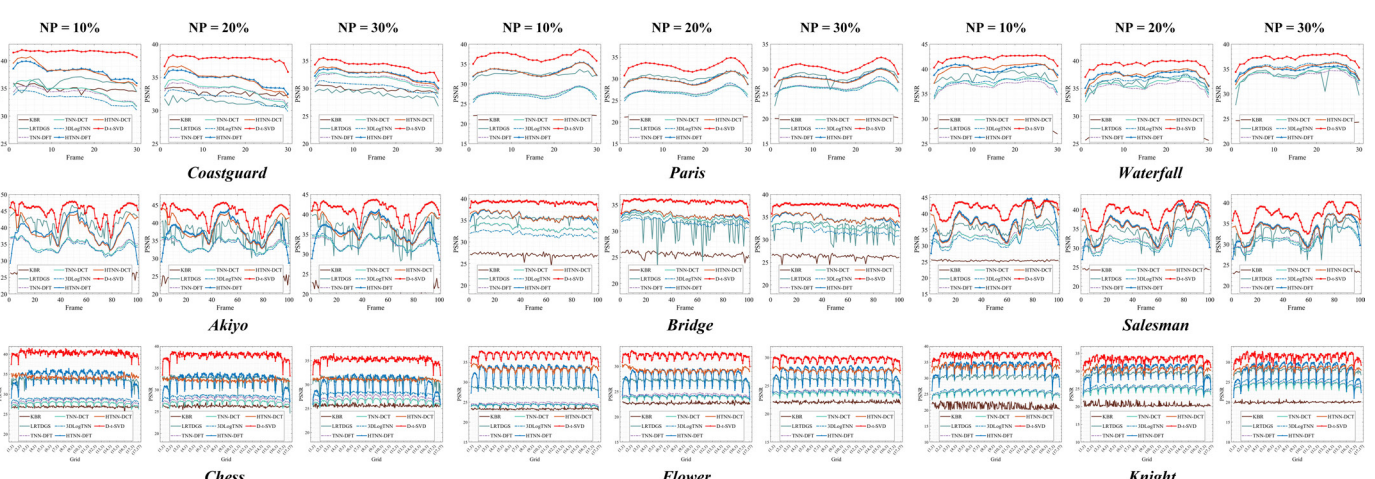


Fig. 17: PSNR as a function of frame/grid RGB images on order-4 **color videos**

TABLE XVII: Quantitative denoising results comparison of all competing **hyperspectral image** denoising methods on *DC Mall* and *Cuprite* with three different cases of Gaussian noise (cases 1-3) and four different cases of mixed noise (cases 4-7).

Dataset	Case	Index	OLRT	NGMeet	NLRCPTD	NLTR	WLRTTR	LRTDGS	3DlogTNN	FRCTR	SDeCNN	FastHyMix	S-WNNM	S-HTNN	S-D-t-SVD
<i>DC Mall</i>	1	PSNR↑	35.009	35.113	32.956	32.820	35.261	33.967	34.010	33.716	32.669	36.089	35.300	35.469	<b>36.561</b>
		SAM↓	0.0642	0.0725	0.0771	0.0711	0.0637	0.0842	0.0707	0.0725	0.1013	0.0606	0.0660	0.0632	<b>0.0565</b>
<i>DC Mall</i>	2	ERGAS↓	4.2480	4.3843	5.3705	5.4441	4.1344	5.2007	4.7373	4.9285	5.7256	3.7564	4.1221	4.0196	<b>3.5605</b>
		PSNR↑	31.832	33.226	30.488	31.518	32.055	31.215	21.342	30.978	29.342	33.462	32.914	32.764	<b>33.776</b>
<i>DC Mall</i>	3	SAM↓	0.0866	0.0777	0.1045	0.0827	0.0931	0.1040	0.4258	0.0948	0.1347	0.0767	0.0798	0.0813	<b>0.0713</b>
		ERGAS↓	6.1217	5.2368	7.0977	6.3194	5.9649	6.5416	23.415	6.7542	8.2018	5.0170	5.3598	5.4519	<b>4.8653</b>
<i>DC Mall</i>	4	PSNR↑	33.310	32.148	31.535	31.833	32.717	32.791	27.369	32.399	31.120	35.142	34.452	34.468	<b>35.514</b>
		SAM↓	0.0771	0.1133	0.0921	0.0789	0.0990	0.0857	0.2742	0.0826	0.1158	0.0660	0.0701	0.0685	<b>0.0619</b>
<i>DC Mall</i>	5	ERGAS↓	5.1561	6.6136	6.3322	6.0967	5.9314	5.4935	15.157	5.7316	6.8032	4.1664	4.5340	4.5016	<b>4.0092</b>
		PSNR↑	31.166	32.477	31.202	31.397	32.093	33.778	33.809	33.149	31.033	34.273	34.534	34.634	<b>35.681</b>
<i>DC Mall</i>	6	SAM↓	0.2062	0.1635	0.1473	0.1427	0.2249	0.0882	0.0758	0.0869	0.1670	0.1295	0.0736	0.0720	<b>0.0638</b>
		ERGAS↓	10.075	7.9729	7.7245	7.6208	10.813	5.1101	4.8759	5.3402	8.5030	6.1185	4.4869	4.4423	<b>3.9429</b>
<i>DC Mall</i>	7	PSNR↑	34.120	34.379	31.471	31.827	33.039	33.430	32.420	32.735	31.975	35.249	35.057	35.069	<b>36.030</b>
		SAM↓	0.0964	0.1016	0.1311	0.1061	0.1387	0.1081	0.1649	0.1054	0.1289	0.0860	0.0691	0.0696	<b>0.0631</b>
<i>DC Mall</i>	8	ERGAS↓	5.2287	5.5593	7.2264	6.4857	7.1132	6.2605	8.4261	6.0956	6.7251	4.5247	4.2242	4.2336	<b>3.8265</b>
		PSNR↑	34.589	34.877	32.272	32.348	34.203	33.835	33.180	33.367	32.391	35.737	35.193	35.143	<b>36.210</b>
<i>DC Mall</i>	9	SAM↓	0.0692	0.0757	0.0857	0.0771	0.0768	0.0887	0.0939	0.0786	0.1059	0.0635	0.0664	0.0642	<b>0.0592</b>
		ERGAS↓	4.5656	4.6164	5.9912	5.8412	5.0320	5.1689	5.6932	5.2006	5.9996	3.9528	4.1847	4.2040	<b>3.7390</b>
<i>DC Mall</i>	10	PSNR↑	31.100	32.329	30.140	30.628	31.750	33.266	31.886	32.079	30.807	33.939	34.299	34.388	<b>35.374</b>
		SAM↓	0.2310	0.1864	0.1898	0.1751	0.2518	0.1085	0.1907	0.1294	0.1960	0.1600	0.0780	0.0762	<b>0.0686</b>
<i>DC Mall</i>	11	ERGAS↓	11.292	9.1695	9.7351	9.1276	12.232	6.2053	9.5881	6.9766	9.9080	7.6111	4.6612	4.6209	<b>4.1357</b>
		PSNR↑	34.075	34.421	32.317	33.210	34.454	33.231	32.957	33.828	32.798	35.239	34.127	34.767	<b>35.839</b>
<i>DC Mall</i>	12	SAM↓	0.0459	0.0474	0.0507	0.0436	0.0434	0.0496	0.0458	0.0451	0.0504	0.0424	0.0453	0.0415	<b>0.0378</b>
		ERGAS↓	3.3464	3.3323	3.9666	3.6182	3.1837	3.6863	3.7697	3.4395	3.7776	3.0139	3.3311	3.0922	<b>2.7794</b>
<i>Cuprite</i>	13	PSNR↑	30.902	32.696	29.741	31.373	31.503	30.518	23.938	31.107	30.507	33.054	31.851	32.063	<b>33.051</b>
		SAM↓	0.0589	0.0509	0.0646	0.0502	0.0575	0.0638	0.1634	0.0556	0.0613	0.0478	0.0535	0.0516	<b>0.0463</b>
<i>Cuprite</i>	14	ERGAS↓	4.6981	3.8845	5.2648	4.4067	4.3490	4.9171	10.933	4.5870	4.8559	3.7232	4.2208	4.1114	<b>3.6941</b>
		PSNR↑	32.462	31.093	30.567	31.706	32.020	31.814	29.200	32.336	31.255	34.436	33.360	33.811	<b>34.723</b>
<i>Cuprite</i>	15	SAM↓	0.0524	0.0733	0.0606	0.0488	0.0592	0.0568	0.0891	0.0505	0.0594	0.0444	0.0494	0.0446	<b>0.0416</b>
		ERGAS↓	3.9600	5.1106	4.8283	4.2527	4.2997	4.2835	6.6337	4.0188	4.5002	3.2545	3.6123	3.4176	<b>3.1221</b>
<i>Cuprite</i>	16	PSNR↑	31.359	31.587	31.369	32.455	32.192	33.025	32.740	33.441	31.717	34.550	33.808	34.175	<b>35.072</b>
		SAM↓	0.0875	0.0809	0.0573	0.0495	0.0865	0.0508	0.0460	0.0465	0.0622	0.0457	0.0465	0.0434	<b>0.0411</b>
<i>Cuprite</i>	17	ERGAS↓	5.6716	5.4010	4.4450	3.9484	5.6122	3.7509	3.8376	3.5725	4.5168	3.2233	3.4258	3.2760	<b>2.9989</b>
		PSNR↑	33.553	34.153	31.941	32.876	33.899	32.959	32.299	33.323	32.501	34.977	33.965	34.485	<b>35.387</b>
<i>Cuprite</i>	18	SAM↓	0.0497	0.0492	0.0551	0.0471	0.0488	0.0517	0.0580	0.0500	0.0530	0.0443	0.0476	0.0442	<b>0.0419</b>
		ERGAS↓	3.5598	3.4015	4.1600	3.7683	3.4444	3.7866	4.2370	3.6651	3.9502	3.0971	3.4121	3.2086	<b>2.9504</b>
<i>Cuprite</i>	19	PSNR↑	33.339	33.620	30.811	31.690	32.449	32.696	31.440	32.841	31.854	34.536	34.110	34.441	<b>35.161</b>
		SAM↓	0.0534	0.0564	0.0688	0.0568	0.0707	0.0594	0.0853	0.0567	0.0665	0.0468	0.0456	0.0422	<b>0.0418</b>
<i>Cuprite</i>	20	ERGAS↓	3.8428	3.8899	5.1465	4.5326	4.9604	4.2576	6.0194	4.0714	4.6934	3.2897	3.3283	3.1988	<b>2.9902</b>
		PSNR↑	30.543	31.234	29.886	30.740	31.407	32.335	30.692	32.165	31.021	34.108	33.246	33.708	<b>34.600</b>
<i>Cuprite</i>	21	SAM↓	0.1122	0.0848	0.0828	0.0678	0.1026	0.0619	0.1004	0.0624	0.0816	0.0497	0.0534	0.0489	<b>0.0461</b>
		ERGAS↓	7.1309	5.5768	5.9557	5.1706	6.6894	4.3878	6.7857	4.4325	5.5885	3.4449	3.7731	3.5571	<b>3.2506</b>

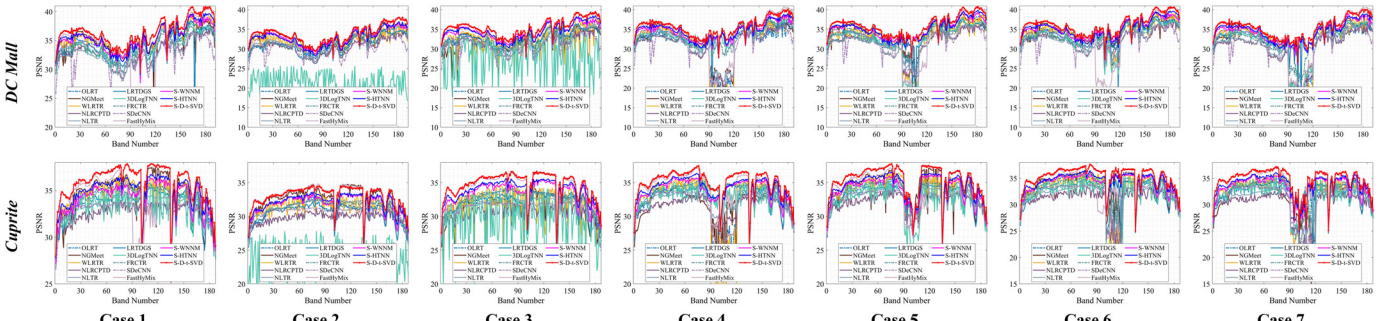
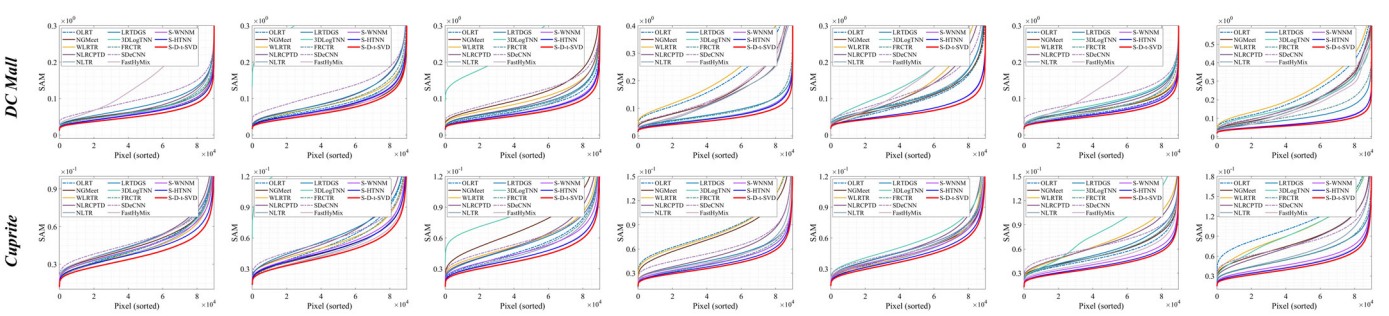


Fig. 18: PSNR as a function of spectral bands on simulated cases 1-7 of the hyperspectral images *DC Mall* and *Cuprite*.



- regularization,” *IEEE Trans. Geosci. Remote Sens.*, vol. 58, no. 1, pp. 734–749, 2019.
- [4] L. Sun, C. He, Y. Zheng, Z. Wu, and B. Jeon, “Tensor cascaded-rank minimization in subspace: A unified regime for hyperspectral image low-level vision,” *IEEE Trans. Image Process.*, vol. 32, pp. 100–115, 2023.
- [5] H. Wang, J. Peng, W. Qin, J. Wang, and D. Meng, “Guaranteed tensor recovery fused low-rankness and smoothness,” *IEEE Trans. Pattern Anal. Mach. Intell.*, vol. 45, no. 9, pp. 10990–11007, 2023.

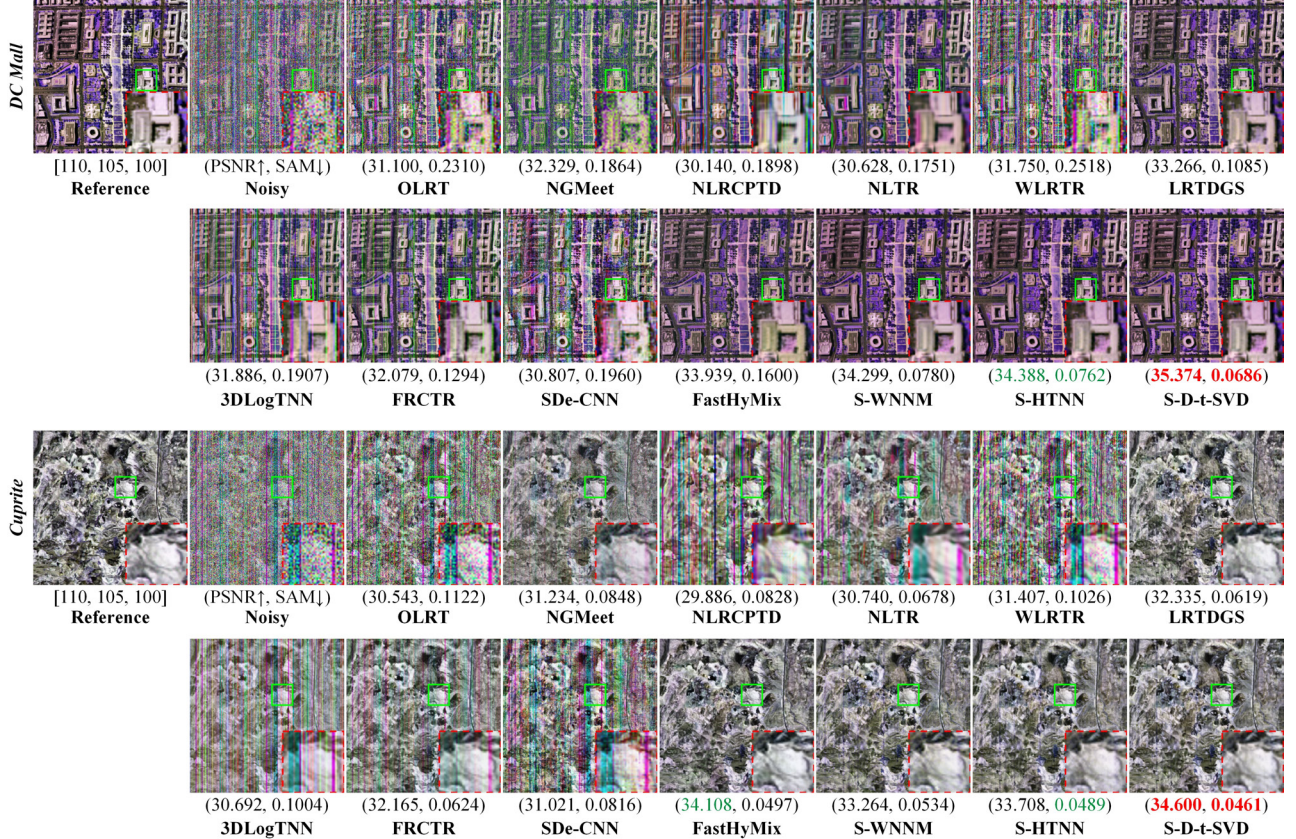


Fig. 20: Mixed denoising results of the most degraded bands on noisy case 7 of two **hyperspectral images**.

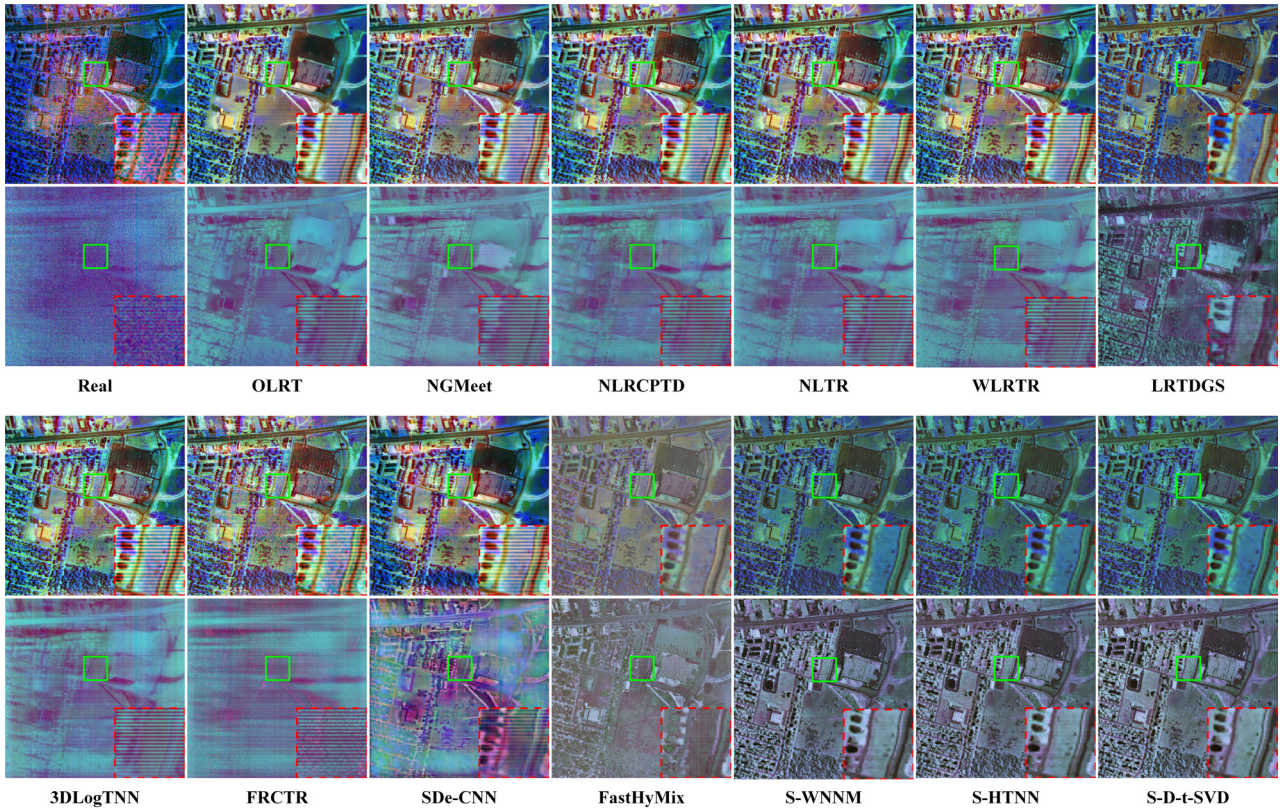


Fig. 21: Denoising results of the most degraded bands of the **real-noisy hyperspectral image** *Urban* (The two rows from top to bottom are composed of bands [210, 140, 105] and bands [150, 138, 87] for each method, respectively).